

# Two successive field-induced spin-flop transitions in single-crystalline $\text{CaCo}_2\text{As}_2$

B. Cheng, B. F. Hu, R. H. Yuan, T. Dong, A. F. Fang, Z. G. Chen, G. Xu, Y. G. Shi, P. Zheng, J. L. Luo, and N. L. Wang  
*Institute of Physics, Chinese Academy of Sciences, Beijing 100080, People's Republic of China*

$\text{CaCo}_2\text{As}_2$ , a  $\text{ThCr}_2\text{Si}_2$ -structure compound, undergoes an antiferromagnetic transition at  $T_N=76\text{K}$  with the magnetic moments being aligned parallel to the  $c$  axis. Electronic transport measurement reveals that the coupling between conducting carriers and magnetic order in  $\text{CaCo}_2\text{As}_2$  is much weaker comparing to the parent compounds of iron pnictide. Applying magnetic field along  $c$  axis induces two successive spin-flop transitions in its magnetic state. The magnetization saturation behaviors with  $\mathbf{H}\parallel c$  and  $\mathbf{H}\parallel ab$  at 10K indicate that the antiferromagnetic coupling along  $c$  direction is very weak. The interlayer antiferromagnetic coupling constant  $J_c$  is estimated to be about 2 meV.

PACS numbers: 75.30.Cr, 75.50.Ee, 75.30.Gw

## I. INTRODUCTION

Magnetic responses of magnetic materials to external fields have been one of the most active fields in condensed matter physics due to their enormous value for fundamental researches and practical applications. Competition between exchange energy, magnetocrystalline anisotropy energy and Zeeman energy could introduce many fascinating magnetic phenomena in magnetic materials.<sup>1,2</sup> Especially, in an antiferromagnet with low anisotropy, a magnetic field applied parallel to the easy axis could induce a transition to a phase in which the magnetic moments lie in a direction perpendicular to the external magnetic field. This is the so-called spin-flop transition. Spin-flop phenomena have been observed in many magnetic materials,<sup>3-6</sup> including many low dimensional antiferromagnets.<sup>7-10</sup>

Recently, the discovery of high- $T_c$  iron pnictide superconductors opens a playground for the community to explore the magnetism and its interplay with superconductivity.<sup>11</sup> Most parent compounds of FeAs-based superconductors exhibit a long-range antiferromagnetic (AFM) order at low temperature. Similar to the cuprates, hole or electron doping will suppress AFM and introduce superconductivity.<sup>12,13</sup> In 1111 family,  $T_c$  reaches up to 55K,<sup>14</sup> which is much higher than the value expected from the traditional electron-phonon coupling theory. It is widely believed that the superconductivity in iron pnictides has an unconventional origin.

Moderate hole or electron doping will destroy the long-range antiferromagnetic order in iron pnictide parents. However, a complete substitution of Fe by Co in  $\text{ReFeAsO}$  ( $\text{Re}=\text{La-Gd}$ ) will introduce complex magnetic phenomena.  $\text{LaCoAsO}$  shows ferromagnetic (FM) order below 55K with saturation moment of  $0.3 \sim 0.4\mu_B$  per Co atom.<sup>15</sup> In  $\text{ReCoAsO}$  ( $\text{Re}=\text{Ce-Gd}$ ), the existence of  $4f$  electrons in rare-earth elements leads to extra complexity in magnetism.<sup>15,16</sup> Recent neutron diffraction experiments reveal  $\text{NdCoAsO}$  undergoes three magnetic transitions: (a) ferromagnetic transition at 69K from Co moments, (b) transition from FM to AFM at 14K and (c) antiferromagnetic order of Nd  $4f$  moments below 1.4K.<sup>17,18</sup> Neutron experiments indicate that all ordered moments lie in the  $ab$  plane. The moments on Co atoms in each CoAs layer are ferromagnetically ordered, and these layers are aligned antiferromagnetically along  $c$  direction. The

two Nd sites in each NdO layer are aligned antiferromagnetically and alternate in direction between layers. The interplay between  $3d$  and  $4f$  electrons may play an important role in these successive magnetic transitions.

However,  $\text{BaCo}_2\text{As}_2$ , which belongs to 122 family, exhibits paramagnetic behavior above 1.8K.<sup>19</sup> The enhancement of susceptibilities relative to the weak correlated electron systems indicates that  $\text{BaCo}_2\text{As}_2$  is close to a magnetic quantum critical point. In this article, we report our exploration of single-crystalline  $\text{CaCo}_2\text{As}_2$ . Different from  $\text{BaCo}_2\text{As}_2$ , we found that  $\text{CaCo}_2\text{As}_2$  undergoes an antiferromagnetic transition at 76K with magnetic moments being aligned parallel to the  $c$  axis. Interestingly, applying magnetic field parallel to the easy axis induces two successive spin-flop transitions in its magnetic state. Our studies indicate that the magnetic coupling between  $ab$  plane is very weak, so that the magnetic ground state of  $\text{CaCo}_2\text{As}_2$  can be disturbed easily by a moderate external magnetic field.

## II. EXPERIMENTAL DETAIL

$\text{CaCo}_2\text{As}_2$  single crystals were grown by a self-flux method similar to the procedures described in many references.<sup>19,20</sup> Typical crystal size was  $\sim 5 \times 5 \times 0.1 \text{ mm}^3$ . Resistivity and specific heat measurements were performed on Quantum De-

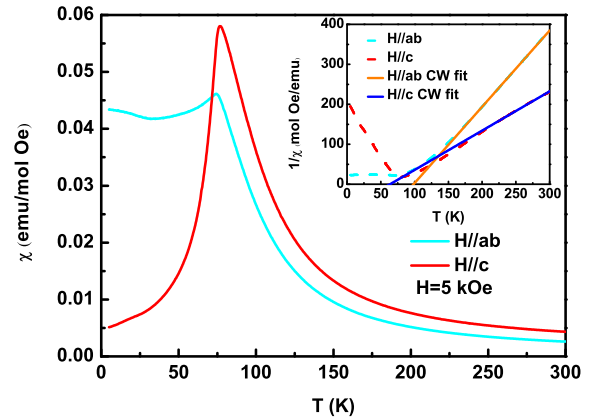


FIG. 1: (color online) Temperature dependent magnetic susceptibilities along  $ab$  plane and  $c$  axis in 5 kOe. The inset is the Curie-Weiss fits to the high temperature parts of susceptibilities.

sign physical property measurement system (PPMS). Dc magnetization was measured as functions of temperature and magnetic field using Quantum Design instrument superconducting quantum interference device (SQUIT-VSM) and PPMS.

### III. RESULTS AND DISCUSSIONS

Figure 1 shows susceptibilities in 5 kOe along the  $c$  axis and  $ab$  plane. The susceptibility for  $\mathbf{H}||c$  exhibits a sharp peak at  $T_N = 76\text{K}$  and drops rapidly with decreasing temperature, indicative of an antiferromagnetic transition with the magnetic moments being aligned parallel to  $c$  axis.<sup>4</sup> Susceptibility for  $\mathbf{H}||ab$  shows a peak around 76K too, but it does not decrease rapidly as  $\mathbf{H}||c$  and shows nearly no temperature dependence below  $T_N$ . Above 150K, the susceptibilities follow the Curie-Weiss law very well. Inset of Fig. 1 shows Curie-Weiss fits to the high temperature parts of susceptibilities. These fits give Weiss temperature  $\theta_{ab}=98\text{K}$  for  $\mathbf{H}||ab$  and  $\theta_c=65\text{K}$  for  $\mathbf{H}||c$ . The effective moment of Co is calculated to be  $1.0\mu_B$  for  $\mathbf{H}||ab$  and  $1.4\mu_B$  for  $\mathbf{H}||c$ . Positive Weiss temperature generally indicates ferromagnetic coupling between the moments. We notice that many compounds with crystal structure similar to  $\text{CaCo}_2\text{As}_2$  show FM ordering in the basal planes, such as  $\text{CaCo}_2\text{P}_2$ ,  $\text{LaCo}_2\text{P}_2$ ,  $\text{CeCo}_2\text{P}_2$ ,  $\text{PrCo}_2\text{P}_2$  and  $\text{NdCo}_2\text{P}_2$ .<sup>21,22</sup> Especially, local-density approximation calculation (LDA) reveals that  $\text{BaCo}_2\text{As}_2$  displays a in-plane ferromagnetic correlation even if it does not exhibit magnetic order above 1.8K.<sup>19</sup> So it is reasonable to infer that the moments of Co atoms are ordered ferromagnetically within  $ab$  plane in its magnetic state. However, the magnetic structure of  $\text{CaCo}_2\text{As}_2$  can not be determined exactly by the static susceptibilities. The simplest supposition of the magnetic structure of  $\text{CaCo}_2\text{As}_2$  is an A-type antiferromagnetism as shown in Fig. 6(a), which means the magnetic moments of Co atoms are aligned antiferromagnetically along the  $c$  axis with the stacking sequence  $+ - + -$ . Another possible type of stacking sequence along  $c$  axis is  $+ + - -$  as shown in Fig. 6(b). This type of stacking se-

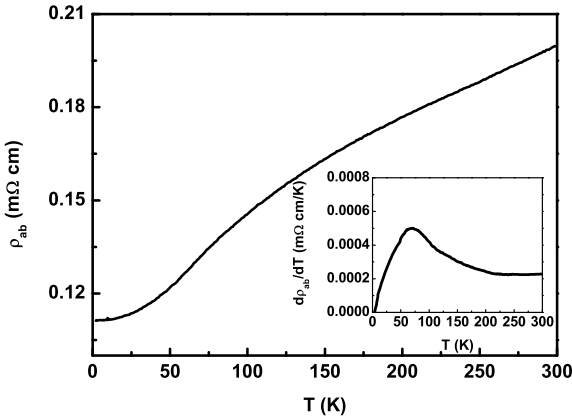


FIG. 2: Temperature dependent resistivity of  $\text{CaCo}_2\text{As}_2$  in zero field with  $\mathbf{H}||ab$ . The inset is the derivative  $d\rho_{ab}/dT$  as a function of temperature.

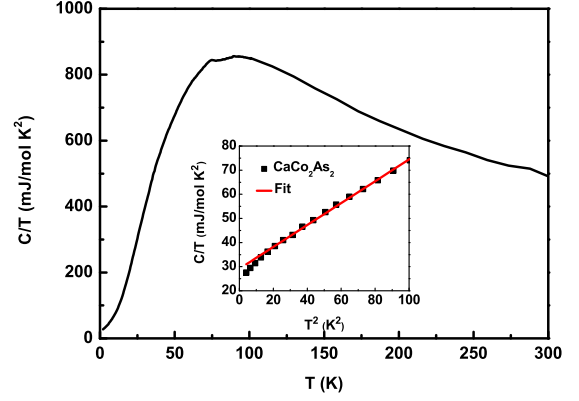


FIG. 3: (color online) Temperature dependence of the specific heat of  $\text{CaCo}_2\text{As}_2$  plotted as  $C/T$  vs  $T$ . The inset is a linear fit to the data below 10K.

quence has been observed in  $\text{PrCo}_2\text{P}_2$  and  $\text{NdCo}_2\text{P}_2$ .<sup>21,22</sup> Neutron experiments are needed to determine the exact magnetic structure of  $\text{CaCo}_2\text{As}_2$ .

Figure 2 shows the resistivity for  $\mathbf{H}||ab$  as a function of temperature.  $\rho_{ab}$  decreases with decreasing temperature, revealing a metallic behavior. There is no clear anomaly in resistivity curve across antiferromagnetic transition temperature. Only a broad peak could be seen in the derivative plot  $d\rho_{ab}/dT$  as shown in the inset of the Fig. 2. This is very different from the electronic transport behaviors of parent compounds of iron-based superconductors, where clear anomalies were observed in resistivity at transition temperature.<sup>12,13</sup> Absence of similar anomaly in  $\rho_{ab}$  of  $\text{CaCo}_2\text{As}_2$  indicates that the coupling between the conducting carriers and antiferromagnetic order in  $\text{CaCo}_2\text{As}_2$  is much weaker than that of iron pnictide parents.

Temperature dependent specific heat is shown in Fig. 3. Although the contribution of phonon specific heat is dominant, we can observe a weak peak locating around 76K clearly. It gives another evidence for a bulk long-range antiferromagnetic transition. The fit to low temperature specific heat data is shown in the inset of Fig. 3. A good linear  $T^2$ -dependent behavior indicates that the low temperature specific heat is mainly contributed by electrons and phonons. The fit yields the electronic coefficient  $\gamma=30\text{ mJ/K}^2/\text{mol CaCo}_2\text{As}_2$  or  $15\text{ mJ/K}^2/\text{mol Co atom}$ . The value, which is much larger than that of iron pnictide parents,<sup>23,24</sup> suggests a high density of states (DOS) at the Fermi level. LDA calculation for  $\text{BaCo}_2\text{As}_2$  reveals that electronic DOS at the Fermi level is already large enough to lead to a mean-field stoner instability toward in-plane ferromagnetism.<sup>19</sup> The large electronic specific heat coefficient of  $\text{CaCo}_2\text{As}_2$  may give us a clue to understand the in-plane ferromagnetism in its antiferromagnetic state.

Magnetic susceptibilities measured in different fields are shown in Fig. 4(a) and 4(b).  $\chi_{ab}(T)$  ( $\chi(T)$  with  $\mathbf{H}||ab$ ) reveals a rather weak field dependence up to 60 kOe. However,  $\chi_c(T)$  ( $\chi(T)$  with  $\mathbf{H}||c$ ) (Fig. 4(b)) shows strong field dependent behaviors. The peak of  $\chi_c(T)$  shifts to low temperature with increasing magnetic field. This is a characteristic feature

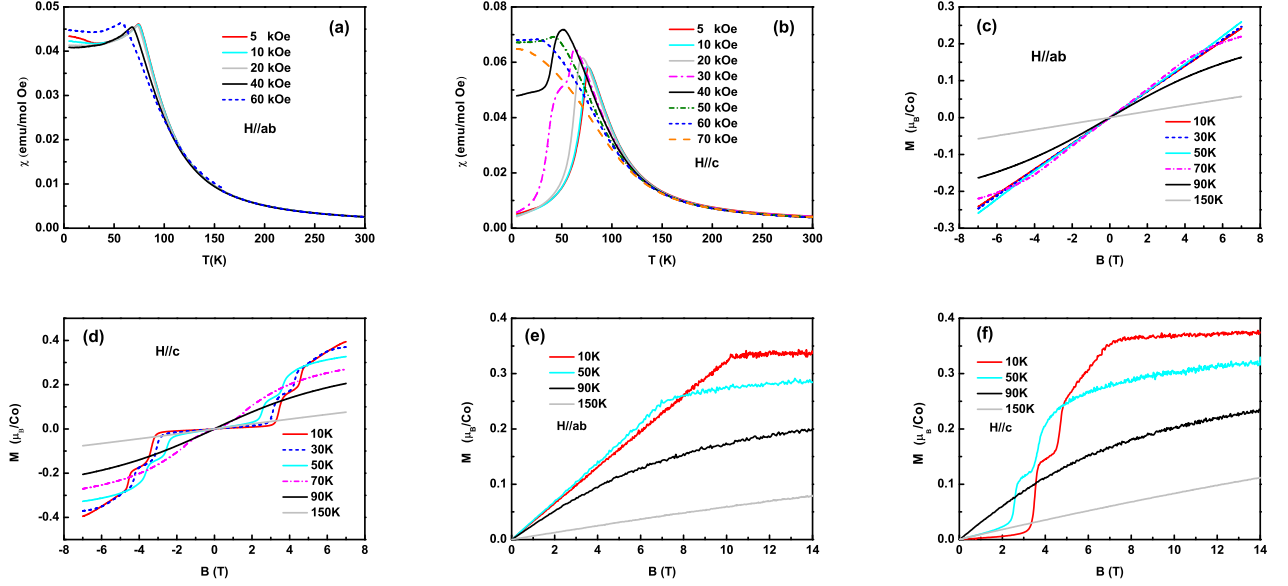


FIG. 4: (color online) (a) and (b) Susceptibilities with  $\mathbf{H} \parallel ab$  and  $\mathbf{H} \parallel c$  in different fields. (c) and (d) Magnetization as a function of field from -7T to 7T below and above  $T_N$  with  $\mathbf{H} \parallel ab$  and  $\mathbf{H} \parallel c$ . (e) and (f) Magnetization as a function of field from 0 to 14T below and above  $T_N$  with  $\mathbf{H} \parallel ab$  and  $\mathbf{H} \parallel c$ .

of antiferromagnetic transition. Below 20 kOe,  $\chi_c(T)$  reveals a well-defined antiferromagnetic transition. However, at  $\mathbf{H}=30$  kOe, a shoulder begins to appear at 50K. With increasing  $\mathbf{H}$ , the low temperature parts of  $\chi_c(T)$  are elevated and a plateau begins to form. At 50 kOe,  $\chi_c(T)$  shows a large plateau below 40K, which indicates that the antiferromagnetic ordering state is heavily disturbed by the applied field. With further increasing magnetic field, the low temperature plateau of  $\chi_c(T)$  is gradually suppressed. At  $\mathbf{H}=70$  kOe, the plateau could not be seen clearly.

To understand these peculiar behaviors of  $\chi_c(T)$ , we collected the magnetization data measured as a function of field above and below  $T_N$ . Figure. 4(c) shows  $\mathbf{M}(\mathbf{H})$  with  $\mathbf{H} \parallel ab$  in the range of -7T to 7T.  $\mathbf{M}_{ab}(10\text{K})$  ( $\mathbf{M}(\mathbf{H}, 10\text{K})$  with  $\mathbf{H} \parallel ab$ ) and  $\mathbf{M}_{ab}(150\text{K})$  exhibit linear increase behavior as a function of applied magnetic field.  $\mathbf{M}_{ab}(\mathbf{H})$  at 70K and 90K deviate from linear behavior slightly. This anomaly originates from the strong magnetic fluctuation around phase transition temperature. Figure. 4(d) gives the results with  $\mathbf{H} \parallel c$ . Different from  $\mathbf{H} \parallel ab$ ,  $\mathbf{M}_c(10\text{K})$  ( $\mathbf{M}(\mathbf{H}, 10\text{K})$  with  $\mathbf{H} \parallel c$ ) undergoes two steep magnetization jumps at  $\mu_0\mathbf{H}_{c1}=3.5\text{T}$  and  $\mu_0\mathbf{H}_{c2}=4.7\text{T}$ . The first jump exhibits a notable hysteresis in the  $\mathbf{M}-\mathbf{H}$  curve as shown in Fig. 5. However, the second one at 4.7T hardly shows a hysteresis. From 5T to 7T, no hysteresis can be observed in  $\mathbf{M}_c(10\text{K})$ . With increasing temperature, the two magnetization jumps become less pronounced and disappear above 70K.  $\mathbf{M}_c(\mathbf{H})$  at 150K shows a good linear behavior as a function of magnetic field, indicating a typical paramagnetic response in paramagnetic states. We noticed that similar steep jump behaviors have been observed in many antiferromagnets, such as  $\text{CuCl}_2 \cdot 2\text{H}_2\text{O}$ ,<sup>3</sup>  $\text{Cu}_2\text{MnSnS}_4$ ,<sup>5</sup>  $\text{BaCu}_2\text{Si}_2\text{O}_7$ ,<sup>7</sup>  $\text{Na}_{0.85}\text{CoO}_2$ <sup>26</sup> and  $\beta\text{-Cu}_2\text{V}_2\text{O}_7$ .<sup>8</sup> A natural explanation to the

steep magnetization jump behaviors in antiferromagnet is a spin-flop transition. To yield more information on the jumps, we performed magnetization measurements up to 14T.

Figure. 4(e) and 4(f) show  $\mathbf{M}_{ab}(\mathbf{H})$  and  $\mathbf{M}_c(\mathbf{H})$  up to 14T at different temperatures. At 10K,  $\mathbf{M}_{ab}(\mathbf{H})$  and  $\mathbf{M}_c(\mathbf{H})$  display moment saturation behaviors at 10.2T and 7.6T respectively. The saturation moments are  $0.33\mu_B$  per Co for  $\mathbf{H} \parallel ab$  and  $0.37\mu_B$  per Co for  $\mathbf{H} \parallel c$ . These values are much smaller than the effective moment per Co atom obtained from Curie-Weiss fits to the susceptibilities, indicative of an itinerant magnetism in  $\text{CaCo}_2\text{As}_2$ . With increasing temperature, the saturation behaviors are weakened and finally disappear above  $T_N$ .

It is well known that spin-flop transition can be induced by a moderate magnetic field in an uniaxial antiferromagnet with low anisotropy. The first jump displays a notable hysteresis

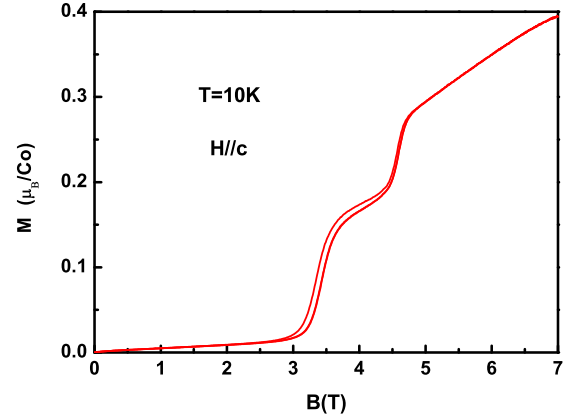


FIG. 5: (color online)  $\mathbf{M}_c$  versus  $\mathbf{H}$  measured up to 7T at 10K with increasing and then decreasing  $\mathbf{H}$

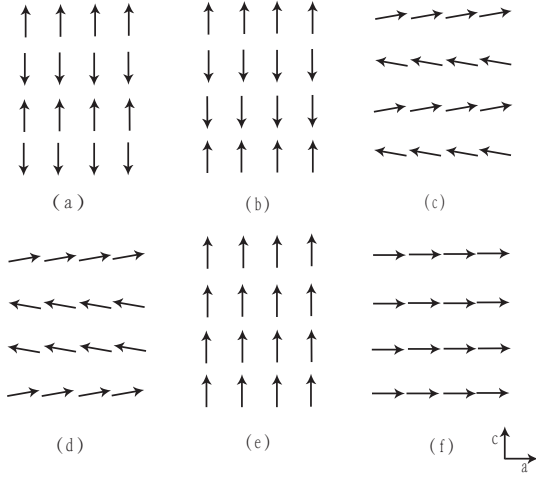


FIG. 6: (a) and (b) Two possible magnetic structures in  $\text{CaCo}_2\text{As}_2$ . (c) and (d) Two possible spin-flop phases in  $\text{CaCo}_2\text{As}_2$ . (e) Arrangement of Co moments in large field with  $\mathbf{H}||c$ . (f) Arrangement of Co moments in large field with  $\mathbf{H}||ab$ .

with increasing and then decreasing  $\mathbf{H}$ , indicating a first-order phase transition. We infer that this jump is ascribed to the traditional spin-flop transition which has been observed in many uniaxial antiferromagnets. The possible magnetic structures of  $\text{CaCo}_2\text{As}_2$  in this spin-flop phase are shown in Fig. 6(c) and 6(d). At 4.7T, another sudden jump occurs in  $\mathbf{M}_c(\mathbf{H})$  at 10K. This jump is unexpected from a simple uniaxial antiferromagnet. The steep increase of magnetization means that the magnetic structure of  $\text{CaCo}_2\text{As}_2$  undergoes a sudden change. Different from the first jump, the second one exhibits much weaker hysteresis behavior. We can not give a detailed description about this spin-flop transition because exact magnetic structure and magnetic interaction in  $\text{CaCo}_2\text{As}_2$  can not be obtained from static susceptibility and magnetization data. We think further neutron experiments are needed to settle this issue. For  $\mathbf{H}||ab$ , behaviors of moments responding to the external field are much simpler than that of  $\mathbf{H}||c$ . The balance between Zeeman energy, antiferromagnetic coupling energy and magnetocrystalline anisotropic energy lead that the magnetic moments are gradually rotated to  $ab$  plane. Above 10.2T, all moments lie in  $ab$  plane and are ordered ferromagnetically as shown in Fig. 6(f).

These interesting magnetic phenomena give us a chance to estimate the antiferromagnetic exchange coupling energy along the  $c$  axis and the magnetocrystalline anisotropic energy in  $\text{CaCo}_2\text{As}_2$ . The behavior of  $\mathbf{M}_c(\mathbf{H})$  in magnetic states is mainly determined by interlayer antiferromagnetic exchange coupling energy  $E_c = \sum_{ij} J_c \mathbf{S}_i \cdot \mathbf{S}_j$  and Zeeman energy  $E_z = -\sum_i \mathbf{m}_i \cdot \mathbf{B}$  and magnetocrystalline anisotropic energy.  $J_c$  is coupling const.  $\mathbf{S}$  and  $\mathbf{m}$  is the spin and moment of Co ions. The saturation behavior above 7.6T in  $\mathbf{M}_c(10\text{K})$  manifests that the moments of Co atoms are all aligned ferromagnetically along the  $c$  axis as shown in Fig. 6(e). At 7.6T, we assume that the energy gain of Zeeman interaction can just overcome the energy cost induced by the antiferromagnetic exchange

coupling when the moments are flipped. In this method, we find a simply approximate relation:  $E_z = -2E_c$  at  $\mu_0\mathbf{H} = 7.6\text{T}$  for  $\mathbf{H}||c$ . Taking the estimated value of  $m \sim 0.4\mu_B$  from the magnetization saturation and assuming  $g=2$ , we estimate  $J_c \sim 2\text{ meV}$ . Neutron scattering data reveal that  $J_c$  in 122 parent compounds of iron-based superconductors varies from 1 meV to 10 meV.<sup>25</sup> Our estimation about  $J_c$  in  $\text{CaCo}_2\text{As}_2$  exhibits the same order of magnitude with 122 parent compounds.

$J_c$  in  $\text{CaCo}_2\text{As}_2$  is much lower than that of some other antiferromagnets, such as  $\text{Na}_{0.85}\text{CoO}_2$ , whose  $J_c$  determined by neutron diffraction is 12.2 meV.<sup>27</sup> In  $\text{Na}_{0.85}\text{CoO}_2$ , a spin-flop transition was observed, which is very similar to the first spin-flop transition in  $\text{CaCo}_2\text{As}_2$ .<sup>26</sup> But up to 14T, the saturated phenomenon of  $\mathbf{M}_c(5\text{K})$  in  $\text{Na}_{0.85}\text{CoO}_2$  had not been observed. This means that  $J_c$  in  $\text{Na}_{0.85}\text{CoO}_2$  is too high for 14T to induce the similar magnetization saturation which occurs in  $\text{CaCo}_2\text{As}_2$ .

The magnetization saturation behaviors for  $\mathbf{H}||ab$  and  $\mathbf{H}||c$  provide some information on the magnetocrystalline anisotropy. That the moments of Co atoms are aligned along the  $c$  axis at zero field indicates that it will cost more energy when the moments lie in  $ab$  plane. To achieve the magnetic state as shown in Fig. 6(e), Zeeman energy must overcome the energy cost caused by magnetic exchange interaction when the moments are flipped. However, to achieve the magnetic state as shown in Fig. 6(f) with  $\mathbf{H}||ab$ , Zeeman energy must overcome extra energy cost induced by magnetocrystalline anisotropic energy. This magnetocrystalline anisotropic energy can be estimated through the difference between the saturation fields of  $\mathbf{H}||ab$  and  $\mathbf{H}||c$ . In this method, the magnetocrystalline anisotropic energy is estimated to be about  $3.76 \times 10^5 \text{ erg/g}$ .

#### IV. SUMMARY

In summary, we have investigated transport and magnetic properties of single-crystalline  $\text{CaCo}_2\text{As}_2$  by means of resistivity, heat capacity, magnetic susceptibility and magnetization measurements. Our results reveal that  $\text{CaCo}_2\text{As}_2$  undergoes an antiferromagnetical transition at  $T_N = 76\text{K}$ . The estimated value of ordered moment on Co atom is about  $0.4\mu_B$ . Two successive spin-flop transitions have been observed at  $\mu_0\mathbf{H}_{c1} = 3.5\text{T}$  and  $\mu_0\mathbf{H}_{c2} = 4.7\text{T}$  in  $\mathbf{M}_c(10\text{K})$ . Our analyses indicate that antiferromagnetic coupling between  $ab$  plane is rather weak. The interlayer antiferromagnetic coupling constant and the magnetocrystalline anisotropic energy are estimated to be about 2 meV and  $3.76 \times 10^5 \text{ erg/g}$  respectively.

#### ACKNOWLEDGMENTS

This work was supported by the National Science Foundation of China (10834013, 11074291) and the 973 project of the Ministry of Science and Technology of China (2011CB921701)

- 
- <sup>1</sup> C. J. Gorter, *Rev. Mod. Phys.* **22**, 277 (1953).
  - <sup>2</sup> A. N. Bodganov, A. V. Zhuravlev, U. K. Röbler, *Phys. Rev. B* **75**, 094425 (2007).
  - <sup>3</sup> C. J. Gorter, *Rev. Mod. Phys.* **25**, 332 (1953).
  - <sup>4</sup> U. Welp, A. Berger, D. J. Miller, V. K. Vlasko-Vlasov, K. E. Gray, and J. F. Mitchell, *Phys. Rev. Lett.* **83**, 4180 (1999).
  - <sup>5</sup> T. Fries, Y. Shapira, Fernando Palacio, M. Carmen Morón, Garry J. McIntyre, R. Kershaw, A. Wold, and E. J. McNiff, Jr, *Phys. Rev. B* **56**, 5424 (1997).
  - <sup>6</sup> Y. Shapira, and S. Foner, *Phys. Rev.* **170**, 503 (1968)
  - <sup>7</sup> I. Tsukada, J. Takeya, T. Masuda, and K. Uchinokura, *Phys. Rev. Lett.* **87**, 127203 (2001).
  - <sup>8</sup> Zhangzhe He, and Yutaka Ueda, *Phys. Rev. B* **77**, 052402 (2008).
  - <sup>9</sup> D. A. Zocco, J. J. Hamlin, T. A. Sayles, M. B. Maple, J. H. Chu and I. R. Fisher, *Phys. Rev. B* **79**, 134428 (2009).
  - <sup>10</sup> R. W. Wang, D. L. Mills, Eric E. Fullerton, J. E. Mattson, and S. D. Bader, *Phys. Rev. Lett.* **72**, 920, (1994)
  - <sup>11</sup> Y. Kamihara, T. Watanabe, M. Hirano, and H. Hosono, *J. Am. Chem. Soc.* **130**, 3296, (2008)
  - <sup>12</sup> G. F. Chen, Z. Li, D. Wu, G. Li, W. Z. Hu, J. Dong, P. Zheng, J. L. Luo, and N. L. Wang, *Phys. Rev. Lett.* **100**, 247002, (2008)
  - <sup>13</sup> Marianne Rotter, Marcus Tegel, and Dirk Johrendt, *Phys. Rev. B* **78**, 020530R, (2008)
  - <sup>14</sup> Z. A. Ren, W. Lu, J. Yang, W. Yi, X. L. Shen, Z. C. Li, G. C. Che, X. L. Dong, L. L. Sun, F. Zhou, and Z. X. Zhao, *Chin. Phys. Lett.* **25**, 2215, (2010)
  - <sup>15</sup> Hiroto Ohta, and Kazuyoshi Yoshimura, *Phys. Rev. B* **80**, 184409, (2009)
  - <sup>16</sup> V. P. S. Awana, I. Nowik, Anand. Pal, K. Yamaura, E. Takayama-Muromachi, and I. Felner, *Phys. Rev. B* **81**, 212501, (2010)
  - <sup>17</sup> Michael A. McGuire, Delphine J. Gout, V. Ovidiu Garlea, Athena S. Sefat, Brian C. Sales, and David Mandrus, *Phys. Rev. B* **81**, 104405, (2009)
  - <sup>18</sup> Andrea Marcinkova, David A. M. Grist, Irene Margiolaki, Thomas C. Hansen, Serena Margadonna, and Jan-Willem G. Bos, *Phys. Rev. B* **81**, 064511, (2010)
  - <sup>19</sup> A. S. Sefat, D. J. Singh, R. Jin, M. A. McGuire, B. C. Sales, and D. Mandrus, *Phys. Rev. B* **79**, 024512, (2009)
  - <sup>20</sup> X. F. Wang, T. Wu, G. Wu, H. Chen, Y. L. Xie, J. J. Ying, Y. J. Yan, R. H. Liu, and X. H. Chen, *Phys. Rev. Lett.* **102**, 117005, (2009)
  - <sup>21</sup> M. Reehuis, W. Jeitschko, G. Kotzyba, B. Zimmer, X. Hu, J. Alloys. comp **266**, (1998), 54
  - <sup>22</sup> M. Reehuis, P. J. Brown, W. Jeitschko, M. H. Möller, and T. Vomhof, *J. Phys. Chem. Solids* **54**, 469, (1993)
  - <sup>23</sup> G. F. Chen, Z. Li, J. Dong, W. Z. Hu, X. D. Zhang, X. H. Song, P. Zheng, N. L. Wang, and J. L. Luo, *Phys. Rev. B* **78**, 224512, (2008)
  - <sup>24</sup> G. F. Chen, W. Z. Hu, J. L. Luo, and N. L. Wang, *Phys. Rev. Lett.* **102**, 227004, (2009)
  - <sup>25</sup> D. C. Johnston, *Advances in Physics* **59**, 803, (2010)
  - <sup>26</sup> J. L. Luo, N. L. Wang, G. T. Liu, D. Wu, X. N. Jing, F. Hu, and T. Xiang, *Phys. Rev. Lett.* **93**, 187203, (2004)
  - <sup>27</sup> L. M. Helme, A. T. Boothroyd, R. Coldea, D. Prabhakaran, A. Stunault, G. J. McIntyre, and N. Kernavanois, *Phys. Rev. B* **73**, 054405, (2006)